

January 1, 2010

Array-Based Sensing of Normal, Cancerous, and Metastatic Cells Using Conjugated Fluorescent Polymers

A Bajaj
OR Miranda
R Phillips
IB Kim
DJ Jerry, et al.



Array-Based Sensing of Normal, Cancerous, and Metastatic Cells Using Conjugated Fluorescent Polymers

Avinash Bajaj,[†] Oscar R. Miranda,[†] Ronnie Phillips,[§] Ik-Bum Kim,[§] D. Joseph Jerry,[‡] Uwe H. F. Bunz,^{*,§} and Vincent M. Rotello^{*,†}

Departments of Chemistry and Veterinary and Animal Science, University of Massachusetts, 710 North Pleasant Street, Amherst, Massachusetts 01003, and School of Chemistry and Biochemistry, Georgia Institute of Technology, 901 Atlantic Drive, Atlanta, Georgia 30332

Received July 22, 2009; E-mail: uwe.bunz@chemistry.gatech.edu; rotello@chem.umass.edu

Abstract: A family of conjugated fluorescent polymers was used to create an array for cell sensing. Fluorescent conjugated polymers with pendant charged residues provided multivalent interactions with cell membranes, allowing the detection of subtle differences between different cell types on the basis of cell surface features. Highly reproducible characteristic patterns were obtained from different cell types as well as from isogenic cell lines, enabling the identification of the cell type as well differentiating between normal, cancerous, and metastatic isogenic cell types with high accuracy.

Introduction

The multivalent capabilities and sensitivity of conjugated polymers to minor conformational or environmental changes make them ideal candidates for biosensing applications.^{1,2} The optical properties of these materials [i.e., absorption (color) and emission (glow)] change significantly in response to even subtle changes in their surroundings. Unlike small-molecule fluorophores, conjugated polymers feature a molecular-wire effect and polyvalent modes of interactions that can enhance signal generation.^{1,2} Moreover, conjugated polymer chains with multiple recognition elements can bind to one analyte molecule, thereby increasing both the binding efficiency and recognition selectivity for specific analytes.³

The favorable properties of conjugated polymers have facilitated their applications in biosensing and bioimaging. As an example, the heparin-like properties of a highly negatively charged poly(*p*-phenyleneethynylene) (PPE) were shown by staining of hamster fibroblast cells, where the PPE selectively binds to fibronectin as a result of significant electrostatic interactions.⁴ Recent studies of cell labeling using polymers^{5,6}

suggest that conjugated polymers could provide an effective platform for cell sensing, including the detection of cancer cells.

Existing methods for cancer cell detection are in general based on antibody array^{7,8} and DNA microarray⁹ techniques and rely on variations in intra- and extracellular protein biomarkers and mutations in the genome, respectively. While antibody-based arrays have been quite successful in early detection of cancers, they require the availability of specific markers for different cancers, a situation that is not the case with many cancers.¹⁰ There is therefore a need for the development of new biosensor strategies for the detection of cancer cells that can distinguish between cell lines on the basis of more subtle differences.

Chemical nose-based sensor array approaches¹¹ that exploit differential receptor–analyte binding interactions provide an alternative to lock-and-key approaches that use specific recognition processes. “Electronic noses/tongues” have been employed for a wide variety of analytes, including metal ions,¹² volatile agents,¹³ aromatic amines,¹⁴ amino acids,¹⁵ carbohydrates,¹⁶ and proteins.¹⁷ While array approaches are quite useful for the

[†] Department of Chemistry, University of Massachusetts.
[‡] Department of Veterinary and Animal Science, University of Massachusetts.

[§] Georgia Institute of Technology.

- (1) Thomas, S. W.; Joly, G. D.; Swager, T. M. *Chem. Rev.* **2007**, *107*, 1339.
- (2) McQuade, D. T.; Pullen, A. E.; Swager, T. M. *Chem. Rev.* **2000**, *100*, 2537.
- (3) (a) Yang, J. S.; Swager, T. M. *J. Am. Chem. Soc.* **1998**, *120*, 11844. (b) Zhou, Q.; Swager, T. M. *J. Am. Chem. Soc.* **1995**, *117*, 12593. (c) Wang, D. L.; Gong, X.; Heeger, P. S.; Rininsland, F.; Bazan, G. C.; Heeger, A. J. *Proc. Natl. Acad. Sci. U.S.A.* **2002**, *99*, 49. (d) Kim, I. B.; Erdogan, B.; Wilson, J. N.; Bunz, U. H. F. *Chem.—Eur. J.* **2004**, *10*, 6247. (e) Kim, I. B.; Bunz, U. H. F. *J. Am. Chem. Soc.* **2006**, *128*, 2818.
- (4) Mcrae, R. L.; Phillips, R. L.; Kim, I. B.; Bunz, U. H. F.; Fahrni, C. J. *J. Am. Chem. Soc.* **2008**, *130*, 7851.
- (5) Kim, I. B.; Shin, H.; Garcia, A. J.; Bunz, U. H. F. *Bioconjugate Chem.* **2007**, *18*, 815.

- (6) Moon, J. H.; McDaniel, W.; MacLean, P.; Hancock, L. E. *Angew. Chem., Int. Ed.* **2007**, *46*, 8223.
- (7) Campagnolo, C.; Meyers, K. J.; Ryan, T.; Atkinson, R. C.; Chen, Y. T.; Scanlan, M. J.; Ritter, G.; Old, L. J.; Batt, C. A. *J. Biochem. Biophys. Methods* **2004**, *61*, 283.
- (8) Wingren, C.; Borrebaeck, C. A. *Curr. Opin. Biotechnol.* **2008**, *18*, 55.
- (9) Petty, R. D.; Nicolson, M. C.; Kerr, K. M.; Collie-Duguid, E.; Murray, G. I. *Clin. Cancer Res.* **2004**, *10*, 3237.
- (10) Crosswell, J. M.; et al. *Ann. Fam. Med.* **2009**, *7*, 212.
- (11) (a) Kim, I.-B.; Han, M. H.; Phillips, R. L.; Samanta, B.; Rotello, V. M.; Zhang, Z. J.; Bunz, U. H. F. *Chem.—Eur. J.* **2009**, *15*, 449. (b) Wang, J.; Liu, B. *Chem. Commun.* **2009**, 2284. (c) Li, H. P.; Bazan, G. C. *Adv. Mater.* **2009**, *21*, 964. (d) Wright, A. T.; Anslyn, E. V. *Chem. Soc. Rev.* **2006**, *35*, 14.
- (12) Lee, J. W.; Lee, J. S.; Chang, Y. T. *Angew. Chem., Int. Ed.* **2006**, *45*, 6485.
- (13) Rakow, N. A.; Suslick, K. S. *Nature* **2000**, *406*, 710.
- (14) Greene, N. T.; Shimizu, K. D. *J. Am. Chem. Soc.* **2005**, *127*, 5695.
- (15) Folmer-Andersen, J. F.; Kitamura, M.; Anslyn, E. V. *J. Am. Chem. Soc.* **2006**, *128*, 5652.
- (16) Buryak, A.; Severin, K. J. *Am. Chem. Soc.* **2005**, *127*, 3700.

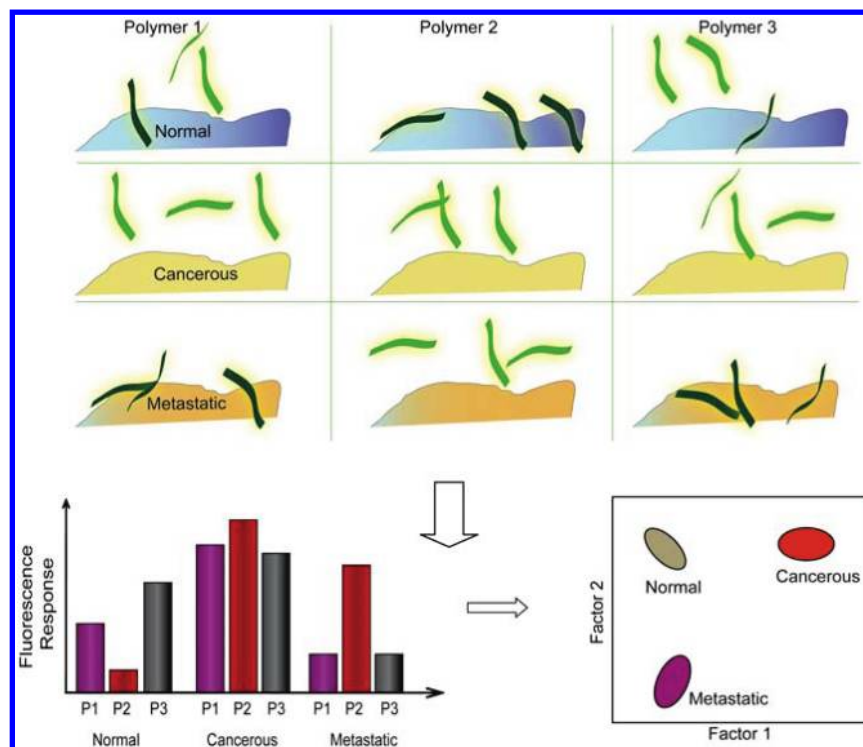


Figure 1. Schematic presentation of the cell detection assay and the interactions between polymers and cell types.

detection of specific analytes, the sensitivity of these systems to subtle changes in analyte ratios makes them particularly promising for cell-sensing applications, as demonstrated by the use of nanoparticle–polymer systems to identify bacteria¹⁸ and mammalian cell types.¹⁹ In this work, we exploited the environmentally responsive fluorescence of PPEs to provide an array-based sensing system (Figure 1) that can differentiate between cell types as well as discern cancerous from noncancerous mammalian cells. Our method uses a differential affinity-based approach as opposed to specific biomarker recognition. The major advantage of this approach is that we do not require knowledge of specific ligands or receptors to differentiate between cell types and states.

Experimental Section

Materials and Methods. Polymers **P1–P8** were synthesized as reported previously.²⁰ The NT2 cell line was obtained from Prof. R. Thomas Zoeller (Biology Department, University of Massachusetts at Amherst). All of the cells were grown in DMEM medium supplemented with 10% fetal bovine serum (FBS) and 1% antibiotics in T75 flasks at 37 °C in a humidified atmosphere containing 5% CO₂. Cells were regularly passaged by trypsinization with 0.1% trypsin (0.02% EDTA, 0.05% dextrose, and 0.1% trypsin) in phosphine-buffered saline (PBS) (pH 7.2).

Cell-Sensing Studies. Cells grown in T75 flasks were washed with DPBS buffer, trypsinized with 1X trypsin, and collected in the DMEM medium. Cells were spun down, resuspended in DMEM medium (without serum proteins/antibiotics), and counted using a hemocytometer. The polymers were dissolved in DPBS buffer (1×) to make 100 nM stock solutions on the basis of their molecular weights. A 200 μ L aliquot of each polymer solution in DPBS was loaded into a well on a 96-well plate (300 μ L Whatman), and the fluorescence intensity values at 465 nm were recorded on a Molecular Devices SpectraMax M5 microplate reader with excitation at 430 nm. Cell suspension (10 μ L, 5000 cells) was added to each well, after which the fluorescence intensity values at 465 nm were recorded again. The ratio of the final fluorescence response after addition of cells to the initial response before cell addition was treated as the fluorescence response. This process was repeated first for four different cancer-cell types to generate six replicates of each. We tested four cell types against the eight-polymer array **P1–P8** six times to generate a training-data matrix of 8 polymers \times 4 cell types \times 6 replicates. Similarly, a training matrix of 8 polymers \times 3 cell types \times 6 replicates was generated for three isogenic cell types. We used the same volume and concentration of DMEM medium for all experiments with various cell types under identical conditions. Therefore, the changes due to the DMEM medium alone would be same for all the experiments.

Linear Discriminant Analysis. The raw data matrix was processed using classical linear discriminant analysis (LDA) in SYSTAT (version 11.0).^{21,22} In the LDA, all of the variables were used in the model (complete mode), and the tolerance was set to 0.001. The raw fluorescence response patterns were transformed to canonical patterns in which the ratio of between-class variance to within-class variance was maximized according to the preassigned grouping. In a blind experiment, the rates of fluorescence patterns of new cases were first converted to canonical scores using discriminate functions established on training samples. The Ma-

- (17) You, C. C.; Miranda, O. R.; Gider, B.; Ghosh, P. S.; Kim, I. B.; Erdogan, B.; Krovi, S. A.; Bunz, U. H. F.; Rotello, V. M. *Nat. Nanotechnol.* **2007**, *2*, 318.
- (18) Phillips, R. L.; Miranda, O. R.; You, C. C.; Rotello, V. M.; Bunz, U. H. F. *Angew. Chem., Int. Ed.* **2008**, *47*, 2590.
- (19) Bajaj, A.; Miranda, O. R.; Kim, I. B.; Phillips, R. L.; Jerry, D. J.; Bunz, U. H. F.; Rotello, V. M. *Proc. Natl. Acad. Sci. U.S.A.* **2009**, *106*, 10912.
- (20) (a) Kim, I.-B.; Dunkhorst, A.; Gilbert, J.; Bunz, U. H. F. *Macromolecules* **2005**, *38*, 4560. (b) Tan, C.-Y.; Pinto, M. R.; Schanze, K. S. *Chem. Commun.* **2002**, 446. (c) Kim, I.-B.; Phillips, R. L.; Bunz, U. H. F. *Macromolecules* **2007**, *40*, 5290. (d) Miranda, O. R.; You, C.-C.; Phillips, R.; Kim, I.-K.; Ghosh, P. S.; Bunz, U. H. F.; Rotello, V. M. *J. Am. Chem. Soc.* **2007**, *129*, 9856.

(21) SYSTAT, version 11.0; Systat Software: Richmond, CA, 2004.

(22) Jurs, P. C.; Bakken, G. A.; McClelland, H. E. *Chem. Rev.* **2000**, *100*, 2649.

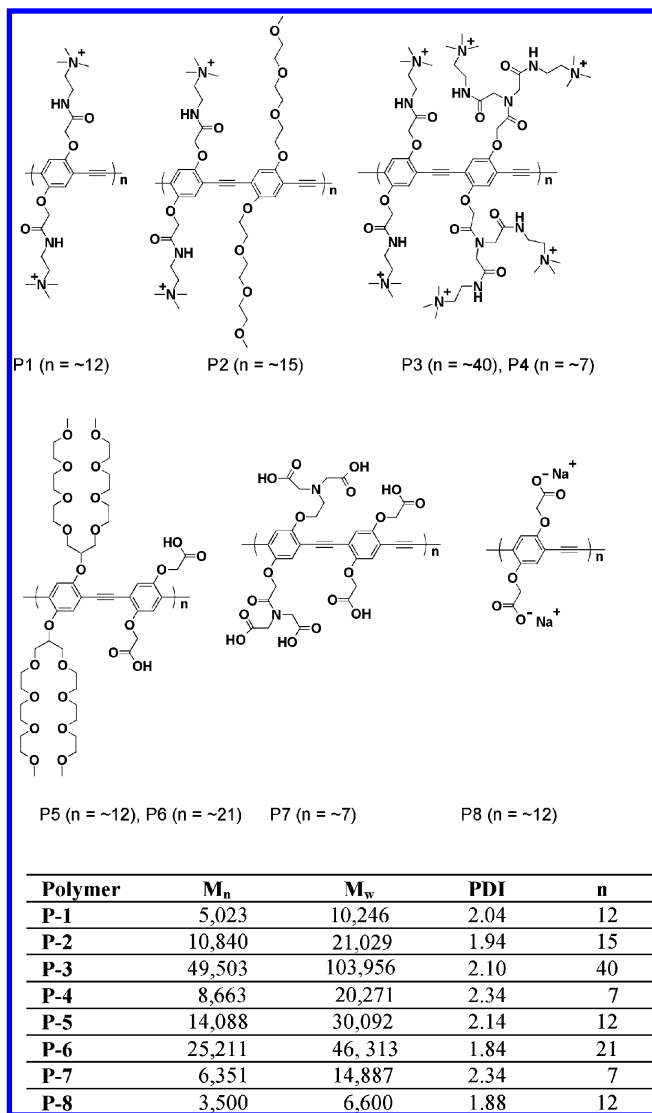


Figure 2. Molecular structures of the fluorescent polymers used in this study.²⁰

halanobis distance,^{23,24} which is the distance of a case to the centroid of a group in a multidimensional space, was calculated for each new case with respect to the centroids of the various groups (normal, cancerous, and metastatic cells) of training samples. The new case was assigned to the group with shortest Mahalanobis distance. This processing protocol was performed using the SYSTAT 11 program, allowing the assignment of cells to specific groups.

Results and Discussion

As a starting point for our studies, we chose eight conjugated fluorescent polymers (Figure 2) based on a common PPE backbone. These PPEs are water-soluble, fluorescent, and structurally diverse, possessing various charge characteristics and differing degrees of polymerization. Our hypothesis was that these characteristics should provide these polymers with selective binding properties and hence differential interactions with different cell surfaces (Figure 1). These differential interactions would involve electrostatic interactions between the cationic/anionic polymers and cell surface functionalities, e.g.,

Table 1. Origin and Nature of the Mammalian Cell Lines Used in This Study

human cell lines	cervix breast liver testis	HeLa MCF-7 HepG2 NT2	cancerous cancerous cancerous cancerous
mouse cell lines	BALB/c mice (breast)	CDBgeo TD V14	normal immortalized cancerous metastatic

lipids, proteins, and polysaccharides. These interactions should lead to different aggregation behaviors of polymers on the cell surfaces, resulting in variation of the polymer fluorescence that could be analyzed by LDA to discriminate different cell types and states.

We selected four different human cancer cell lines and three isogenic cell lines for our studies (Table 1). Each of these cell types has a different function that would be expected to be manifested in surface functionality in practice. The isogenic breast cell lines provide a particularly valid testbed for our sensor array, as these cells differ only in cell state, providing a model for detection of cancer in clinical settings.

In practice, we first titrated the polymers with different concentrations of cell suspensions to determine the sensitivity of the array. The fluorescence titration studies showed the required sensitivity using 5×10^3 cells (see the Supporting Information), indicating that the final concentration of cells should be 5×10^3 cells/210 μ L. In all subsequent experiments, this concentration of cells was used. The fluorescence of the PPE solution (100 nM, on the basis of number-average molecular weight) in PBS was recorded. Next, 5×10^3 cells in 10 μ L of DMEM medium was added to the PPE solution, and the mixture was incubated for 30 min, after which the fluorescence of the polymer was recorded again. The experiments were performed for each of the eight polymers with six replicates. The fluorescence response patterns were generated from the ratios of final and initial fluorescence of the polymers. The fluorescence intensities of all of the samples decreased upon exposure to the mammalian cells because of polyvalent interactions of the polymers with the cell surfaces. To sort out the fluorescence responses that provide the discriminating signatures, we classified the fluorescence data set for all eight polymers using classical LDA as implemented in the SYSTAT software (version 11). This statistical analysis method is used to recognize the linear combination of features that differentiate two or more classes of objects or events. Stepwise analysis with different polymer set(s) (i.e., Jackknifed classification) was used to determine which polymer set could best differentiate between the cells. The *Jackknifed classification matrix* is an attempt to approximate cross-validation. The Jackknifed classification matrix uses functions computed from all of the data except the case being classified. Figure 3 presents the Jackknifed classification matrix for all of the different sets of cell lines using different combinations of polymers. As demonstrated in Figure 3, we were able to pick out different combinations by logically ruling out the cases that led to less separation. Then we considered the combinations containing the least number of polymers. We observed the maximum differentiation grouping using four common polymers (**P2**, **P2**, **P3**, and **P5**) in the present study. Next, we subjected the data obtained from different cancer cell types and isogenic cell lines to LDA using these common set of particles to determine the separation within each class (see below).

(23) Mahalanobis, P. C. *Proc. Natl. Inst. Sci. India* **1936**, 2, 49.

(24) Gnanadesikan, R.; Kettenring, J. R. *Biometrics* **1972**, 28, 81.

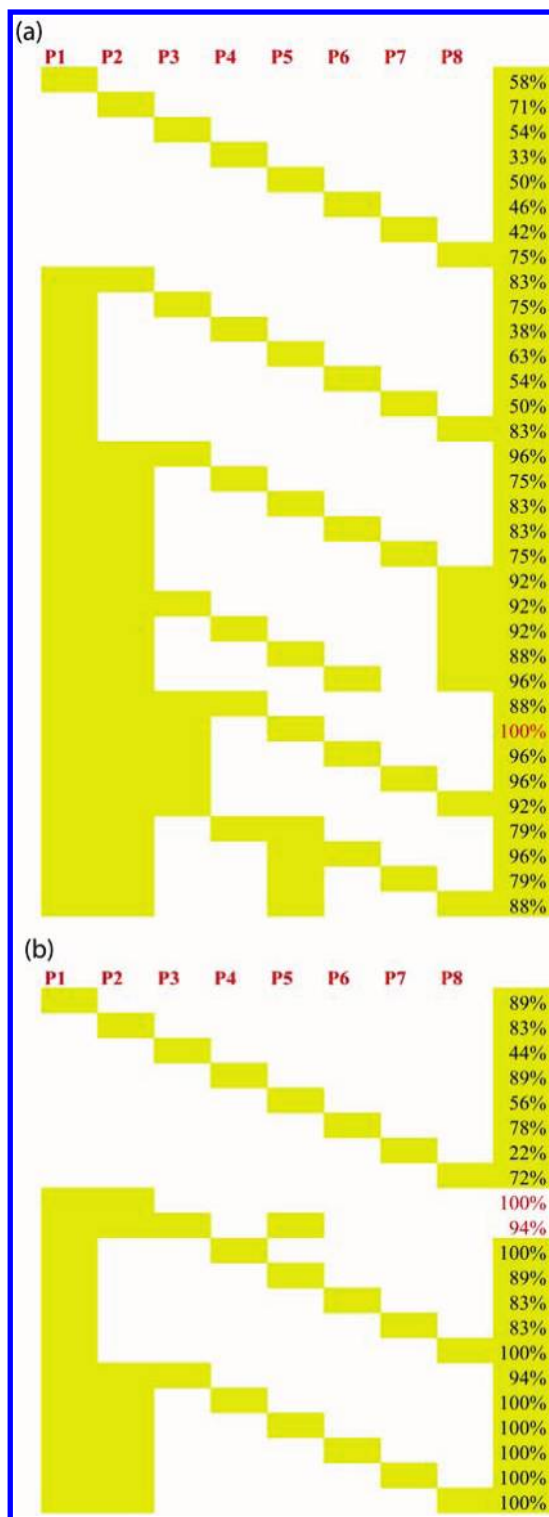


Figure 3. Jackknifed classification matrix obtained using LDA for eight polymers for (a) the four cell lines HeLa, MCF-7, NT2, and HepG2 and (b) the three cell lines CDBgeo, TD, and V14.

Figure 4a presents the fluorescence response of the four cell lines (HeLa, MCF-7, NT2, and HepG2) to polymers **P1**, **P2**, **P3**, and **P5**. LDA converted the patterns of the training matrix (4 polymers \times 4 cell lines \times 6 replicates) to canonical scores. The first three canonical factors contained 96.7, 3.0, and 0.3% variance, as shown in Figure 4b. In this plot, each point represents the response pattern for a single cell type to the polymer sensor array. In the canonical fluorescence response

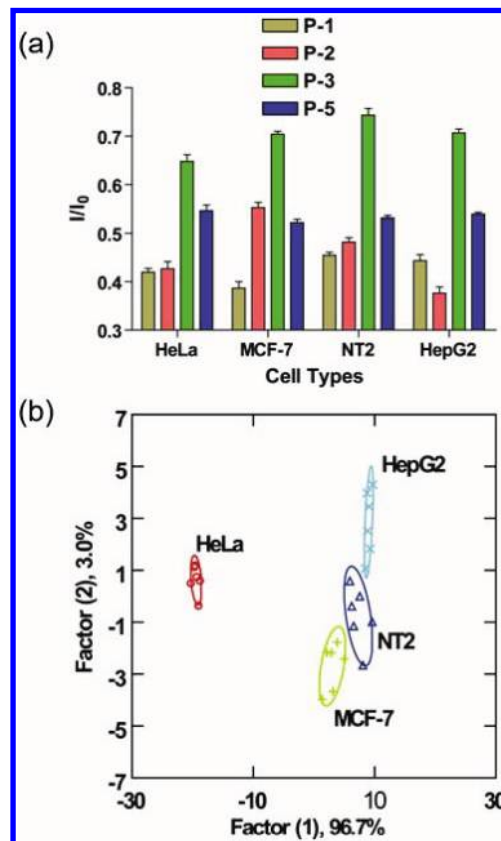


Figure 4. (a) Fluorescence responses of four different cancer cell lines [HeLa (cervical), MCF7 (breast), HepG2 (liver), and NT2 (testes)] using fluorescent polymers. Each value is the average of six parallel measurements. (b) Canonical score plot for two factors of simplified fluorescence response patterns obtained with the fluorescent polymer arrays.

patterns, the different cell types are clustered into four non-overlapping groups (95% confidence level ellipses) (Figure 4b), indicating the ability of this set of polymers to differentiate between the four different cancer cell types using a simple polymer array.

These initial results validate our ability to differentiate cell types phenotypically on the basis of their surface properties. A much more challenging goal is to differentiate cells on the basis of cell state, i.e., to differentiate between genetically identical healthy, cancerous, and metastatic cells. To determine the ability of our sensors to detect and identify cancer, we used three cell lines from genetically identical BALB/c mice (Table 1). CDBgeo cells were prepared by retroviral infection with a marker gene encoding the fusion of β -galactosidase and neomycin resistance. These cells exhibited normal outgrowths when transplanted into mammary fat pads. The TD cells were prepared by treating CDBgeo cells with 10 ng/mL TGF- β for 14 days,²⁵ and withdrawal for five passages resulted in a persistent epithelial-to-mesenchymal transformation: tumorigenic growth resulted upon transplantation. The V14 cell line was established from a primary mammary tumor arising in BALB/c-Trp53 \pm mice.²⁶ The cells lack p53 protein and form aggressive tumors that are locally invasive in mice. Therefore, the CDBgeo, TD, and V14 cells differ from each other by just

(25) Deugnier, M. A.; Faraldo, M. M.; Teuliere, J.; Thierry, J. P.; Medina, D.; Glukhova, M. A. *Dev. Biol.* **2006**, *293*, 414.

(26) Blackburn, A. C.; McLary, S. C.; Naeem, R.; Luszcz, J.; Stockton, D. W.; Donehower, L. A.; Mohammed, M.; Mailhes, J. B.; Soferr, T.; Naber, S. P.; Otis, C. N.; Jerry, D. J. *Cancer Res.* **2004**, *64*, 5140.

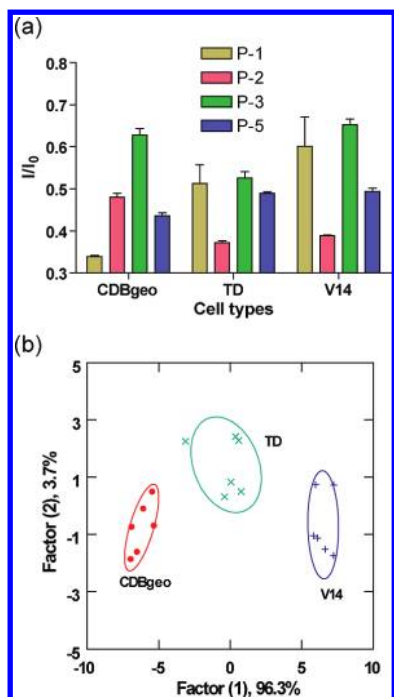


Figure 5. (a) Fluorescence responses of the three isogenic cell lines CDBgeo, TD, and V14 using polymer arrays. Each value is the average of six parallel measurements. (b) Canonical score plot for the first two factors of simplified fluorescence response patterns obtained with polymer arrays against different mammalian cell types. The canonical scores were calculated by LDA for identification of the three cell lines.

a single cell-state transformation. As an example, V14 is different from CDBgeo and TD in lacking only the p53 tumor suppressor gene.

The three cell lines (CDBgeo, TD, and V14) were screened with the eight PPEs; the Jackknifed analysis (Figure 3b) indicates that optimal differentiation (94%) was achieved using the same four polymers as before, i.e., **P1**, **P2**, **P3**, and **P5**. Figure 5a shows the fluorescence patterns obtained from the four polymers **P1**, **P2**, **P3**, and **P5** upon their incubation with the isogenic cell types. These patterns were reproducible and subjected to LDA (Figure 5b) to generate the training matrix of 4 polymers \times 3 cell types \times 6 replicates having the first two factors of 96.3 and 3.7% variance, respectively, with 94% accuracy. Therefore, using this array-based approach, we can discriminate the subtle changes between different cell states, providing a model for cancer detection in clinical applications.

The robustness of the polymer array system was tested using unknowns generated from the three isogenic cell lines. The fluorescence response patterns generated were subjected to LDA, during which the cell types were classified into the groups generated through the training matrix according to the shortest of their Mahalanobis distances to the respective groups. In these studies, we observed 80% accuracy of the unknown samples (19 out of 24).

Analysis of the combined results indicates that four polymers (**P1**, **P2**, **P3**, and **P5**) out of the original eight could distinguish different mammalian cells effectively. Of the four polymers, **P1–P3** are cationic and would hence be expected to interact with the negatively charged cell membrane. Significantly, polymer length is important, as **P3** and **P4** have the same structure but only the longer **P3** was effective at differentiation, suggesting that polyvalency is an important consideration in differentiation. Polymers **P5–P8** are anionic in nature, and the nature of their interactions with the cells is not clear. It is worth noting, however, that the least-charged anionic polymer (**P5**) was the most effective at cell differentiation.

Conclusions

In summary, we have developed a conjugated fluorescent polymer-based sensor array using PPE polymers and demonstrated its utility in cell sensing. Using this sensor array, we can distinguish between several cancer cell types as well as between isogenic healthy, cancerous, and metastatic cells that possess the same genetic background. Taken together, these studies provide an effective sensor for differentiating cell types as well as a potential direction in the creation of polymer-based imaging agents and delivery vehicles based on differential cell interactions. Thus, “nose”-based polymer sensor arrays represent a new method for diagnostic, biophysical, and surface science processes involving cell surfaces.

Acknowledgment. We thank Professor R. Thomas Zoeller (Biology Department, University of Massachusetts at Amherst) for providing the NT2 cell lines. This work was supported by the NSF Center for Hierarchical Manufacturing at the University of Massachusetts (DMI-0531171); NIH Grants GM077173 (to V.M.R.) and AI073425, CA095164, and CA105452 (to D.J.J.); and Department of Energy Grant DE-FG02-04ER46141 (to U.H.F.B. and V.M.R.)

Supporting Information Available: Complete ref 10, fluorescence titration data, and results for unknown samples. This material is available free of charge via the Internet at <http://pubs.acs.org>.

JA9061272